

FAINT FIELD GALAXIES: AN EXPLANATION OF THE FAINT BLUE EXCESS USING NUMBER EVOLUTION MODELS

PING HE^{1,2}, ZHEN-LONG ZOU^{1,2}, AND YUAN-ZHONG ZHANG^{2,3}

¹Beijing Astronomical Observatory, National Astronomical Observatory, Chinese Academy of Sciences, Beijing 100012, P.R. China, and CAS-PKU Joint Beijing Astrophysics Center, Beijing 100871, P.R. China (hemm@itp.ac.cn)

²Institute of Theoretical Physics, Academia Sinica, P.O.Box 2735, Beijing 100080, P.R.China

³CCAST (World Laboratory), P.O.Box 8730, Beijing 100080, P.R.China

Draft version October 23, 2018

ABSTRACT

Pure luminosity evolution models for galaxies provide an unacceptable fit to the redshifts and colors of faint galaxies. In this paper we demonstrate, using HST morphological number counts derived both from the I_{814} -band of WFPC2 in the Medium Deep Survey (MDS) and the Hubble Deep Field (HDF) and from the $H_{1.6}$ -band of NICMOS, and ground-based spectroscopic data of the Hawaii Deep Field and the Canada-France Redshift Survey, that number evolution is necessary for galaxies, regardless of whether the cosmic geometry is flat, open, or Λ -dominated. Furthermore, we show that the number evolution is small at redshifts of $z < 1$, but large at $z > 1$, and that this conclusion is valid for all the three cosmological models under consideration. If the universe is open or Λ -dominated, the models, which are subject to the constraint of the conservation of the comoving mass density of galaxies, naturally predict a population of star-forming galaxies with the redshift distribution peaking at $z = 2 \sim 3$, which seems to be consistent with the recent findings from Lyman-break photometric selection techniques. If the cosmological model is flat, however, the conservation of the comoving mass density is invalid. Hence, in order to account for the steep slope of B -band number counts at faint magnitudes in the flat universe, such a star-forming galaxy population has to be introduced ad hoc into the modelling alongside the merger assumption.

1. INTRODUCTION

The origin and nature of the excess population of faint blue galaxies (FBG) has been a topic of intense debate for many years (Koo & Kron 1992; Ellis 1997). The number counts of galaxies at blue (B , $\lambda_{eff}=4500$ Å) and near-infrared (K , $\lambda_{eff}=2.2$ μ m) wavelengths produce conflicting results. The B -band counts show an excess over the no-evolution predictions, and suggest strong luminosity evolution in galaxy populations, while the K -band counts are well fitted by models with only passive evolution. When spectroscopic samples are available, it is found that the redshift distributions of galaxies are also consistent with passive evolution while strong luminosity evolution will lead to a high- z distribution, in excess of the observations. To avoid these paradoxes, a number of scenarios have been suggested. The first is pure luminosity evolution (PLE) in galaxy populations, which increases the distance to which galaxies may be seen (Tinsley 1980; Bruzual & Kron 1980; Koo 1981, 1985; Guiderdoni & Rocca-Volmerange 1990; Gronwall & Koo 1995; Pozzetti, Bruzual, & Zamorani 1996). The

second attempt is the choice of a cosmological geometry that maximizes the available volume, either by adopting a low value of the deceleration parameter q_0 (an open cosmological model) or by introducing a cosmological constant λ_0 (Broadhurst, Ellis & Shanks 1988; Colless et al. 1990; Cowie, Songaila & Hu 1991; Colless et al. 1993; Fukugita et al. 1990). The third is to increase the number of galaxies at earlier times, either by introducing additional populations, which once existed at high z but have since disappeared or self-destructed (Broadhurst, Ellis, & Shanks 1988; Cowie 1991; Babul & Rees 1992; Babul & Ferguson 1996; Ferguson & Babul 1998), or by merging, that is by assuming that present-day galaxies were in smaller fragments at high redshifts (Rocca-Volmerange & Guiderdoni 1990; Cowie et al. 1991; Guiderdoni & Rocca-Volmerange 1991; Broadhurst, Ellis & Glazebrook 1992; Carlberg & Charlot 1992; Kauffmann, Guiderdoni & White 1994; Roukema et al. 1997).

One constraint on the nature and evolutionary behavior of faint galaxies arises from the morphological number counts derived from the Hubble Space

Telescope (HST), whose unprecedented imaging ability enables galaxies to be segregated morphologically into several broad classes (Glazebrook et al. 1995a; Driver et al. 1995; Abraham et al. 1996; Teplitz et al. 1998). These morphological data have provided us with valuable information to understand the origin and evolution of galaxies. Now, any self-consistent theory of galaxy evolution and cosmology must pass the test of matching the distribution of galaxy properties derived from HST morphological data.

In a previous investigation (He & Zhang 1998, hereafter HZ98), we modelled the number counts of E/S0 galaxies obtained from the MDS and the HDF in the HST I_{814} -bandpass ($\lambda_{eff}=8000\text{\AA}$), and found that the number counts of ellipticals could be well explained by PLE models in any cosmological model if ellipticals are assumed to have formed at high redshifts (say $z_f=5.0$) and thereafter have passively evolved (i.e., no further star formation). This is just the traditional scenario of the formation and evolution for elliptical galaxies. However, incorporating other observations such as redshift and color distributions and the modelling of the other types (i.e., early- and late-type spirals and irregulars, as separated by HST), we have found that the FBG problem cannot be resolved by the conventional scenario for elliptical galaxies, and the inclusion of dust extinction also cannot save the scenario. This conclusion holds in each of the three cosmological models under consideration: flat, open and Λ -dominated. Our investigation suggests that number evolution may be essential to explain the faint data (He & Zhang 1999a, hereafter HZ99a).

Number evolution models have been widely considered to account for the paradoxes concerning the FBG problem, whereas PLE model is the starting point of our investigation. We model the number counts of the three classes of galaxies- ellipticals, early-type spirals, and late-type spirals/irregulars- which are derived from the HST I_{814} -passband, and in combination with the analysis of redshift distributions in the observed magnitude bins, we find that PLE models can explain the number counts at the bright magnitudes of $I_{814} < 22.5$. This indicates that PLE models could be valid up to $z \sim 1$, in apparent contradiction to scenarios of strong number evolution at low redshifts (e.g., Kauffmann, Charlot, & White 1996). Kauffmann et al. concluded that only one third the number of nearby bright elliptical galaxies were in place at $z \sim 1$, which would seem to be inconsistent with the number counts at the bright end. Our conclusion is consistent with those of Roukema & Yoshii (1993) and Woods & Fahlman (1997) based on the analysis of angular correlation function, and that of Totani & Yoshii (1998) based on the V/V_{max} anal-

ysis (Schmidt 1968), and in particular, agrees well with the results of Im et al. (1999), based on the morphologically divided redshift distribution of faint galaxies, and those of Brinchmann et al. (1998) and Lilly et al. (1998), based on the HST imaging of the CFRS and LDSS redshift surveys.

We tentatively construct a set of phenomenological number-luminosity evolution (NLE) models to explain data such as the morphological number counts in both the I_{814} -band of the Wide Field and Planetary Camera 2 (WFPC2) and the $H_{1.6}$ -band of the Near-Infrared Camera and Multiobject Spectrometer (NICMOS), as well as the counts in B - and K -bands derived from most of the ground-based observations and redshift distributions derived from the Hawaii sample (Cowie et al. 1996) and the Canada-France Redshift Survey (CFRS) (Lilly et al. 1995a). The significant feature of these models is that the number evolution is small at redshifts of $z < 1$, while it is large at high redshifts. We find that NLE models can roughly reproduce these observations.

To simplify the modelling, we employ the constraint of conservation of the comoving mass density of galaxies, in the form of Guiderdoni & Rocca-Volmerange (1991). We find that a population of late-type spiral/irregular galaxies and star-forming galaxies naturally emerge in our models, due to mass conservation. Such a population will peak at $z \approx 2.8 - 3$. Between $z \sim 3$ and the present day, it behaves as a population which seems to be fading, disappearing or self-destructing, with very blue colours. Such a population also seems to be consistent with the recent findings using Lyman-break selection techniques (see Steidel & Hamilton 1992, 1993; Steidel, Pettini, & Hamilton 1995; Madau 1995). This conclusion, however, is only valid in open (e.g., $\Omega_0=0.1$) or Λ -dominated (e.g., $\Omega_0=0.2$, $\lambda_0=0.8$) cosmological models. If the universe is flat ($\Omega_0=1$), the comoving mass density of such a predicted population becomes negative at high redshifts ($z > 3$), which is physically unreasonable. Therefore, to account for the faint data, we abandon the constraint of mass conservation and introduce a star-forming population *ad hoc* into the modelling.

In Section 2, we present the PLE models. We are particularly interested in the behaviors of the models at bright magnitudes, or at low redshifts. Section 3 is devoted to the number evolution models. The summary and conclusions are presented in Section 4.

2. PURE LUMINOSITY EVOLUTION

PLE model is the starting point of the investigation. This kind of model takes as ingredients the stellar evolutionary tracks, normally for a restricted metallicity range, the initial mass function (IMF),

and a gas consumption timescale associated with star formation rate (SFR), which are adjusted to give the present range of colors across the Hubble sequence. With each galaxy assumed to evolve as an isolated system, the rest-frame spectral energy distribution (SED) can be predicted at a given time and thus an evolutionary correction can be determined (Ellis 1997). The evolutionary SEDs of galaxies are computed using population synthesis models, (e.g., the latest Bruzual & Charlot synthesis code, which we employ in this work). The reader is referred to HZ98, HZ99a or Pozzetti et al. (1996) for details of the modelling. We also consider the effects of dust extinction, following Wang's (1991) prescription, which is similar to that of HZ98 and HZ99a. However we choose a larger optical depth of $\tau^* = 0.3$ than that adopted by Wang for galaxies other than ellipticals (see also Campos & Shanks 1997).

Similar to the prescription of HZ98 and HZ99a, we adopt three representative cosmological models in this work: 1) flat, $\Omega_0 = 1.0$, $\lambda_0 = 0$, and $h = 0.5$ ($H_0 = 100 h \text{ km s}^{-1} \text{ Mpc}^{-1}$) (hereafter, Scenario A), 2) open, $\Omega_0 = 0.1$, $\lambda_0 = 0$, and $h = 0.5$ (Scenario B), and 3) flat and Λ -dominated, $\Omega_0 = 0.2$, $\lambda_0 = 0.8$, and $h = 0.6$ (Scenario C). We assume a formation redshift $z_f = 5.0$ for all types of galaxies in all three cosmological models.

We first consider the modelling of the morphological number counts derived from the MDS and the HDF in the I_{814} -passband. The basic ingredient of the models, the present-day luminosity function (LF), is not well-determined by local surveys due to inherent uncertainties such as a large local fluctuation (Shanks 1989), significant local evolution (Maddox et al. 1990a), selection effects and/or incompleteness (Zwicky 1957; Disney 1976; Ferguson & McGaugh 1995), or perhaps systematic errors in local surveys (Metcalfe, Fong & Shanks 1995a). Therefore, a simple 3 parameter Schechter function (ϕ^* , M^* and α , cf., Schechter 1976), as adopted by most authors, seems not to be universal, and hence not to be quite appropriate as an average over all types and environments (cf., Binggeli, Sandage, & Tammann 1988). In particular, much recent work finds a tail for dwarfs and late types that is steeper than $\alpha \sim -1.3$ (Driver, Windhorst & Griffiths 1995), and in addition, low surface brightness galaxies (LSBGs) may make up a significant amount of the luminosity density of the local universe (see Impey & Bothun 1997 for a review about LSBGs). Regardless of these uncertainties, the simple Schechter form for local LFs is still our working assumption in the current research.

Firstly, we adjust the Schechter LF parameters by trial and error so that the model predictions can match better the bright-end number counts, since the

count normalization is sensitive to the three parameters ϕ^* , M^* and α , especially the former two (cf. Ellis 1997). The LFs for galaxies are listed in Table 1. Secondly, we test these ad hoc adoptions by comparison with observations. It can be seen, in Figure 1, that both the B - and the K -band adopted LFs lie close to the observations, and in particular, the observed faint-end slopes are not as high as, say -1.5, as predicted by the semi-analytic models (cf. Cole et al. 1994; Kauffmann, White & Guiderdoni 1993).

2.1. Number counts for elliptical galaxies

We adopt the Scalo (1986) IMF for ellipticals and the Salpeter (1955) IMF for the other types. As addressed in HZ98, the Scalo IMF is less rich in massive stars than the Salpeter IMF because of the steeper slope of the former at the high-mass end. The SFR for ellipticals is adopted as the simple exponential form

$$\psi(t) \sim \exp(-t/\tau_e), \quad (1)$$

where $\psi(t)$ refers to the SFR, and τ_e is the timescale characterizing this kind of SFR. A single value of τ_e can not satisfactorily reproduce the $B - K$ color distribution (He & Zhang 1999b), which may be a reflection of intrinsic complexities such as the metallicity variations among the population of ellipticals. Besides, there is also an age-metallicity degeneracy (Worthey 1994), which greatly complicates the situation. For the sake of simplicity, we neglect the chemical evolution in the current work. In our models, ellipticals are subdivided into five parts equal in number, with each one of them specified by a different τ_e for SFR to characterize its luminosity evolution. By such treatments, we hope to circumvent the metallicity-age degeneracy. The values of τ_e , modelled $B - I$ and $B - K$ colors are shown in Table 2. Notice that the observed average $B - K$ color for present-day ellipticals is ~ 4.10 (Johnson photometric system), with the dispersion being about 0.1–0.2 mag, and hence these values of the parameter τ_e are acceptable. It is well known that the local photometric and spectroscopic properties of ellipticals are largely insensitive to the past star formation history (cf. Bruzual 1983; Bower, Lucey & Ellis 1992; Charlot & Silk 1994).

We show in Fig.2-(a) the predicted number counts for ellipticals by PLE models to compare with those derived from HST in I_{814} -passband. It can be seen that up to $I_{814} = 22.5$, the predictions can satisfactorily reproduce the bright-end number counts in all the three scenarios, indicating the PLE models are valid within this magnitude range. At the faint-end ($I_{814} > 22.5$), however, the predictions in Scenarios B and C largely overestimate the observations. Although the prediction for Scenario A fits the bright

counts well, as we have analyzed in HZ99a, models with strong luminosity evolution predict too many high- z objects, in substantial disagreement with the color-selected sample from Cowie et al. (1996).

Though PLE models are unacceptable, we present redshift distributions for ellipticals in the observed I_{814} magnitude bins, in order to better understand the models. In Fig.2-(b), (c) and (d), we show predictions of redshift distributions in the three magnitude bins, $I_{814} < 21.0$, $21.0 < I_{814} < 22.5$, and $22.5 < I_{814} < 25.0$. The redshift distributions peak around $z \sim 0.5$, indicating the counts at $I_{814} < 21.0$ are contributed by the objects at the redshifts of $z < 0.5$ or even as large as $z \sim 0.8$ (the half maximum of the peaks), and from Fig.2-(c), it can be seen that the peaks appear at $z \sim 0.8$, indicating the objects between $21.0 < I_{814} < 22.5$ are mostly at $z < 0.8$ or ~ 1.0 . From the previous analysis, we know that the number counts at $I_{814} < 22.5$ can be well explained by PLE models up to $z \sim 1$. As addressed above, the predicted number counts at $I_{814} > 22.5$ in Scenarios B and C significantly exceed the observations, and from Fig.2-(d), we know that these excessive objects mostly lie in $z \geq 1$. This implies, for example, that if a merger scenario for the evolution of ellipticals is involved, then the merger rate in the interval $0 < z < 1$ seems to be small. This conclusion is valid in all the three world models under consideration.

We now consider an example of strong number evolution for ellipticals. Kauffmann, Charlot & White (1996) claimed, based on $\langle V/V_{max} \rangle$ analysis (Schmidt 1968) and the data from the CFRS and the Hawaii Deep Survey (Cowie et al. 1996), that only one third of the nearby bright elliptical galaxies existed at $z \sim 1$. We adopt their expression of the number density evolution for ellipticals with respect to z , i.e., $F = (1+z)^{-\gamma}$, with $\gamma = 1.5 \pm 0.4$ (This means $F \approx 1/3$ at $z = 1$), to compare the predictions with observations. We show the model predictions in Fig.2-(a). Obviously, such a strong number evolution cannot be accepted, since it underestimates the bright-end number counts. Notice that the bright-end counts are mostly contributed by L^* galaxies, and hence they are insensitive to the LF faint-end slope α . An enhancement of the normalization ϕ^* by, say 50% can improve the goodness of fit, but such an enhancement will produce too many bright ellipticals at the present day, and conflict with the local surveys, especially the LF at K -band. It is worthy of mentioning that Totani & Yoshii (1998) have performed a detailed V/V_{max} test, and concluded that the value of $\langle V/V_{max} \rangle$ for ellipticals is ~ 0.5 in the redshift range $0.3 < z < 0.8$, which means that the number density is nearly unchanged in this redshift range, and this conclusion is similar to ours. We con-

clude that strong number evolution for ellipticals at low redshifts is not acceptable.

2.2. Number counts for early-type spiral galaxies

Using the morphological classification of galaxies by HST, we combine Sab and Sbc galaxies into a group of early-type spirals. The LFs are presented in Table 1. The SFR is taken the same exponential form as Eq. [1], but the timescales are generally larger than those of ellipticals in order to match their local photometric properties. These parameters are listed in Table 2.

In Fig.3-(a), we present our PLE model predictions of number counts to compare with the observations. The models satisfactorily reproduce the observations at almost all magnitudes in Scenarios B and C, indicating little number evolution. For Scenario A, however, the PLE model cannot account for observations at $I_{814} > 22.5$, and hence other assumptions than PLE are needed. As is Section 2.1, we analyze the redshift distributions in the observed magnitude bins.

We can see from Fig.3-(b) and (c) that, in the magnitude bins $I_{814} < 21.0$ and $21.0 < I_{814} < 22.5$, there are peaks in the redshift distributions at $z \approx 0.5 \sim 0.8$, indicating that PLE models could be valid even out to the redshift of the half maximum of the peaks, i.e., $z \approx 0.8 \sim 1.0$. For $I_{814} > 22.5$, we can see from Fig.3-(d) that the models fail to predict enough early-type spirals at the redshifts of $z > 1.0$.

2.3. Number counts for late-type spiral/irregular galaxies

We mix Scd and Sdm/Irr classes into a category of late-type spiral/irregular galaxies. In addition, we introduce another population which has very blue colors (even bluer than irregular galaxies), and we refer to it as the vB galaxies with the name taken after Pozzetti et al. (1996). The vB galaxies are included to explain the bluest colours, $B - K \approx 2$ of the Hawaii sample and $(V - I)_{AB} \approx 0.5$ of the CFRS sample. As addressed by Totani & Yoshii (1998), such very blue galaxies comprise nearly 10% of the CFRS sample. The very blue colors suggest that they are star-forming galaxies, and hence vB galaxies are meant to reproduce the population of star-burst galaxies present at each z , whose evolution does not follow the prescription of standard population synthesis. Following the treatment of Pozzetti et al., we assume that star formation in these galaxies keeps their SEDs constant in time, and the SEDs can be approximated by a model with constant SFR lasting 1.5 Gyr.

Their LFs are also listed in Table 1. In Fig.4-(a), we show the predicted number counts for comparison with observations. Similar to the cases of ellipticals

and early-type spirals, the PLE models can also reproduce the late-type spiral/irregular population to $I_{814} < 22.5$, indicating that PLE models could be valid in the redshift range $z < 0.8 \sim 1$ (Fig.4-(b) and (c)), while at $I_{814} > 22.5$, especially for Scenario A, the models underpredict the observations, indicating the models need to be improved at high redshifts of $z > 1$ (Fig.4-(d)).

In short, PLE models can well explain the number counts of all types of galaxies at the magnitudes of $I_{814} < 22.5$, or equivalently, according to the analysis of redshift distributions, at the redshifts of $z < 1$. Hence, strong number evolution at low redshifts is not acceptable, comparing to the observations.

3. NUMBER-LUMINOSITY EVOLUTION

Pure luminosity evolution works fairly well at low redshifts, $z < 1$, as suggested by our previous investigations. Next, without considering the underlying physical mechanism, we phenomenologically construct a set of number evolution models to explain the faint data. There is no doubt that the luminosity evolution must occur, due to the aging of star populations. Moreover, if mergers between galaxies are included in the modelling, it is more realistic to consider the additional star formation, that can be induced by interactions between galaxies. For simplicity, we use the same galaxy evolution models as in Section 2 to compute the K -corrections and evolutionary-corrections for galaxies, without considering more complicated star formation scenarios (e.g., Colín, Schramm, & Peimbert 1994; Fritze-v.Alvensleben & Gerhard 1994), or various complicated physical processes concerning the formation of galaxies (cf. Roukema et al. 1997).

Number evolution can be simply realized by making the LF parameters ϕ^* , M^* and α functions of z . For this, we adopt the following expressions:

$$\phi^*(z) = \phi_0^* (1+z)^{Q_0+Q_2 z^2}, \quad (2)$$

where ϕ_0^* refers to the characteristic density of present-day galaxies. Q_0 and Q_2 are two free parameters. This form is a refinement of our previous formalism (cf. HZ99a), and can also be treated as a modification of that of Guiderdoni & Rocca-Volmerange (1991), in which the power-law index is not a function of z . Obviously, Q_2 will mostly affect the high- z behavior. The evolution of the faint-end slope α is parametrized as the following:

$$\alpha(z) = \alpha_0 - \gamma_1 \left(\frac{z}{z_f} \right) - \gamma_2 \left(\frac{z}{z_f} \right)^2, \quad (3)$$

where α_0 represents the local quantity, and z_f is the formation redshift. The two parameters γ_1 and γ_2

characterize the functional relationship between α and z . In principle, M^* should also be a function of z . We find, however, the variation of M^* can be to some extent compensated by that of ϕ^* and α , and for simplicity, we neglect the variation of the characteristic magnitude. Our model is therefore similar to the $\phi^* \cdot \alpha$ model of Guiderdoni & Rocca-Volmerange (1991).

Thus we have four free parameters, Q_0 , Q_2 , γ_1 and γ_2 , with which to characterize the number evolution. Nevertheless, for a specific Hubble type, there is no need to invoke simultaneously all the four parameters. Our strategy to proceed is to involve as few of these parameters as possible, as long as the models can reproduce the observed data. We model the three Hubble types independently.

3.1. Morphological number counts

We first consider the explanation of elliptical number counts by the NLE models. From Section 2, we realize that the number evolution is small at $z < 1$, hence the (absolute) value of the parameter Q_0 should be low. Since the PLE predictions exceed the observations at faint magnitudes (i.e., at high redshifts), the parameter Q_2 should be negative. We try to fix these two parameters by trial and error to match the data. It can be seen from Panel (a) of Figure 5, that the NLE models can reproduce well the data at both bright and faint magnitudes in each of the three Scenarios. The values of Q_0 and Q_2 are listed in Table 3, and in Figure 6, we show the relationship of ϕ^* with z . We can see that the number density of ellipticals is nearly unchanged in the redshift range of $z < 1$; while at high redshifts, ellipticals are absent regardless of the cosmological models. This conclusion agrees well with the finding of Totani & Yoshii (1998) based on the V/V_{max} analysis, and is also in agreement with that of Zepf (1997).

The number counts of early-type spirals can also be satisfactorily reproduced by our models (See Panel (b) of Figure 5). For Scenarios B and C, only γ_1 and γ_2 are needed, and Q_0 or Q_2 is not necessary. There are additional advantages for such α -variation models, that the faint-end counts are contributed by dwarfs rather than bright galaxies, and hence there are no high- z tails predicted by the models. For Scenario A, it seems that Q_2 is also needed, since the flat universe has less volume at high redshifts than the open or Λ -dominated universe, and hence a slightly positive Q_2 can help to improve the fit at faint magnitudes. The values of these parameters are also listed in Table 3. We can see that the variation of α at low redshifts is also not dramatically large. For example, α steepens only by 0.06 from $z = 0$ to $z = 1$ in Scenario A.

The modelling for the late-type spiral/irregular and vB galaxies is similar to that for ellipticals and early-type spirals, but requires even more free parameters. As a result, we proceed in an alternative way. In a scenario of hierarchical clustering, galaxies are constantly merging over cosmic time. If the hierarchical picture is realistic, and in the absence of other scenarios such as fading or self-destructing of a galaxy population, then the total comoving masses of gas and stars can be regarded to be enclosed within galaxies. Hence the total comoving mass density should be conserved in merger processes. We employ the conservation of mass to constrain the number density evolution of the latest Hubble types.

Mass (baryonic, including gas and stars) conservation can be expressed in the following way:

$$\sum_j M_j^*(z) \phi_j^*(z) \Gamma(\alpha_j(z) + 2) = \text{constant}, \quad (4)$$

which is taken from Guiderdoni & Rocca-Volmerange (1991). M^* is the characteristic mass of the galaxy mass function (MF). The total mass density is computed by summing over galaxy type j , and the constant can be determined by present-day quantities. In order to obtain the evolution of LFs, we need to convert the evolving MFs into evolving LFs, and hence the mass-to-luminosity (M/L) ratios are needed. Unfortunately, the M/L ratios are poorly determined, especially for B -passband. However, the near-infrared light is less affected by star formation, and thus by evolution, than the optical emission, and it is a good tracer of the total mass within galaxies. Hence we will make use of K -band LFs instead of the MFs of galaxies.

We assume the faint-end slope α for late-type galaxies (Scd, Sdm/Irr, and vB) evolves in the same way as for the early-type spirals (Sab and Sbc). In this case the evolution of ϕ^* can be determined by Eq. [4]. The evolution of the characteristic number density ϕ^* for L^* galaxies is illustrated in Figure 7. We first analyze the cases for Scenarios B and C. Using the constraint of mass conservation suggested by Eq. [4], ϕ^* increases with increasing z to the maximum at $z \sim 2.8$ in both Scenarios B and C, and then decreases to almost zero at the formation redshift z_f . At $z = 1$, the number density ϕ^* for L^* galaxies is 44% and 88% higher than the present-day value for Scenarios B and C, respectively. Notice that the Sdm/Irr/vB galaxies are star-forming galaxies, as suggested by their blue colors and predicted by our population synthesis models. If we only focus on these galaxies, they appear to be a disappearing or self-destructing population (cf. Babul & Rees 1992; Babul & Ferguson 1996; Ferguson & Babul 1998), but they are produced naturally by the merger scenario,

and are not needed to be ad hoc introduced into the models. In particular, since the faint-end slope α also increases with z , there are even more dwarf galaxies at high redshifts. Such a population seems to be qualitatively consistent with the recent findings using Lyman-break selection techniques (see Steidel & Hamilton 1992, 1993; Steidel, Pettini, & Hamilton 1995; Madau 1995) that a substantial population of star-forming galaxies exists at $z \geq 3$ (Steidel et al. 1996; Steidel et al. 1998). We believe that such a population of Lyman-break galaxies can be identified with the Sdm/Irr/vB galaxies suggested by our models.

Such an analysis, however, cannot be applied to the case of Scenario A. In Figure 7, ϕ^* becomes negative when $z > 3$, which is obviously unphysical. The reason why ϕ becomes negative at high redshifts is that a flat universe has less volume at a given redshift than an open or Λ -dominated universe. Therefore, in order to account for the faint-end counts, the number evolution of early-type spirals for Scenario A has to be larger than that for Scenarios B and C (See Table 3). On the other hand, the number evolution of ellipticals for Scenario A is less than for Scenarios B and C. As a result, the increase of the mass density for early-type spirals exceeds the corresponding decrease for ellipticals. Therefore, if the model is subject to the constraint of the mass density conservation, it will inevitably predict a negative ϕ^* for Sdm/Irr/vB galaxies at high-redshifts. The implication is that the mass density conservation suggested by Eq. [4] cannot be applied to the case of Scenario A, and furthermore, in order to explain the faint data, the mass density must increase with z .

The failure of the assumption of mass density conservation in Scenario A can be understood in several different ways, and its cosmological interpretation is also not unique. There may be a disappearing/self-destructing population of star-forming galaxies at high redshift which has no present-day counterpart. Another possibility is that galaxies have been losing mass during their evolution, in particular, during the period of merging between galaxies, due to supernovae which enable the gas to escape from the potential well of dark matter halos. The situations may be very complicated.

Regardless of the difficulty in explaining the physical mechanism behind the non-conservation of the mass density for galaxies, we can follow the same ad hoc prescription as that for early-type spirals to adjust the parameters (Q_0, Q_2, γ_1 , and γ_2) of the models to match the data, without discriminating between the two possibilities discussed above. The values of these parameters are also listed in Table 3. The predicted number counts for the latest type galaxies are

shown in Panel (c) of Figure 5. It can be seen that the predictions can be accepted within the uncertainties. In addition, the predictions for the overall population (shown in Panel (d) of Figure 5) are also acceptable.

The morphological number counts in the near-infrared bands have also been provided by NICMOS (Teplitz et al. 1998). Predictions of the NLE models are presented in Figure 8 to compare with the observed data in the $H_{1.6}$ band ($\lambda_{eff} = 1.6\mu m$). We can see that the models can reasonably reproduce the data.

3.2. Number counts in B - and K - passbands

We now examine whether the number evolution models can reproduce B - and K -bands number counts obtained from the majority of surveys so far. From Figure 9 we can see that the models can reproduce better the number counts at bright magnitudes in both the B ($B < 21$) and the K ($K < 17$) bands, indicating that the normalization (involving both ϕ_0^* and L^* , cf. Ellis 1997) is appropriate using the adopted LFs. (Due to large uncertainties in the local LFs, the normalizations are usually chosen to scale the model predictions to the observed number counts at a relatively faint magnitude of $B \sim 19.0$. See Pozzetti et al. 1996 for a comprehensive review). Furthermore, the NLE models can reproduce the counts at the faintest B and K magnitudes for each of the three Scenarios.

3.3. Redshift distribution

The spectroscopic studies with the LRIS spectrograph on the Keck Telescope of two of the Hawaii deep survey fields SSA 13 and SSA 22 (Cowie et al. 1996) and the CFRS present two of the largest and deepest redshift samples so far, providing powerful tools for understanding the evolution of galaxies.

In Fig.10-(a), (b), and (c), we show the predicted z -distributions in the magnitude range of $22.5 < B < 24.0$ in the three Scenarios, to compare with measured redshifts from Cowie et al. (1996), whose completeness is more than 85%. We can see that the predictions roughly match the observed data, and in particular, there are no very high- z tails. In Fig.10-(d), (e), and (f), we compare the NLE-model predicted z -distributions, limited in the magnitude range of $17.5 < I_{AB} < 22.5$, with the CFRS sample (Lilly et al. 1995a; Le Fèvre et al. 1995; Lilly et al. 1995b; Hammer et al. 1995; Crampton et al. 1995). Notice that the CFRS data are less deep than the Hawaii sample, with the completeness $\sim 85\%$. We can see that the predictions are reasonably matched by the data, especially for Scenarios B and C. However, we should also realize that all models overpredict galaxies with $z > 1$. The overprediction may be due to

the z -unidentified galaxies, since the completeness of both of the two samples is around 85%, and, according to Pozzetti et al., such z -unidentified galaxies are most probably at high z (see Section 3.6 of Pozzetti et al. 1996).

4. SUMMARY AND CONCLUSIONS

Recent morphological data on faint galaxies are of great significance for us in understanding the distant universe, and have shed new light on the long-standing FBG problem. We have systematically investigated this question using HST data. In previous work, we found that the number counts of ellipticals could be explained successfully by PLE models only a scenario where ellipticals have *extremely* short SFR timescales ($\tau_e = 0.2, 0$, and 0.05 Gyr for flat, open and Λ -dominated universes, respectively), i.e., they formed at high- z (say $z_f = 5$) and have passively evolved since their formation (HZ98). Such a view, however, would contradict other observations such as color distributions (HZ99a). Hence, the evolution of galaxy number density seems to be required, and one of the main purposes of this work is to study the nature of the number evolution.

PLE models are the starting point of our investigation. By modelling the number counts of the three morphological classes in the HST I_{814} -passband, in combination with the analysis of redshift distributions in the three observed magnitude bins, $I_{814} < 21.0$, $21.0 < I_{814} < 22.5$, and $22.5 < I_{814} < 25.0$, we find that PLE models can fit the number counts at the bright magnitudes of $I_{814} < 22.5$, indicating such PLE models could be valid up to $z \approx 1$. As a result, scenarios of strong number evolution at low redshifts such as that of Kauffmann et al. (1996) would seem to be rejected. The results agree well with those of Im et al. (1999), based on the morphologically divided redshift distribution of faint galaxies, and those of Brinchmann et al. (1998) and Lilly et al. (1998), based on the HST imaging of the CFRS and LDSS redshift surveys. In addition, our conclusions are also consistent with those of Roukema & Yoshii (1993) and Woods & Fahlman (1997) based on analysis of the angular correlation function, and that of Totani & Yoshii (1998) based on the V/V_{max} analysis.

We then constructed a set of phenomenological number-luminosity evolution models and by trial and error fixed a set of model parameters to explain the data such as morphological number counts both in I_{814} - and in $H_{1.6}$ -bands, as well as the counts in the B - and K -bands, and redshift distributions derived from the Hawaii and the CFRS samples. The significant feature of these models is that the number evolution is small at redshifts of $z < 1$ and large at higher redshifts. We find that the models can roughly

reproduce the above-mentioned observations in each of the cosmologies under consideration.

To simplify the modelling, we employ the constraint of conservation of the comoving mass density of galaxies, in the form presented by Guiderdoni & Rocca-Volmerange (1991). We find that a population of late-type spiral/irregular galaxies and very blue galaxies naturally emerge in these models. Such a population will peak at $z \approx 2.8$. We argue that such a population seems to be consistent with the recent findings using Lyman-break photometric selection techniques. This conclusion, however, is only valid in an open or Λ -dominated cosmological models. If the universe is flat, the comoving number density of such a predicted population becomes negative at high redshifts ($z > 3$), and hence it is obviously physically unacceptable. Therefore, in order to account for the faint data, such a population has to be introduced ad hoc into the modelling. The failure of the mass conservation assumption in a flat universe model, as discussed in Section 3.1, may imply the existence of a disappearing/self-destructing population of star-forming galaxies at high redshifts, whose present-day counterpart is not detectable. Alternatively, galaxies may have been losing mass during their lifetimes, due to supernova bursts, for exam-

ple. If so, the evolutionary scenario for galaxies may be extremely complicated.

We have not taken into account the evolution of metallicity with redshift, and details such as the recycling of the residual gas ejected by dying stars. These would be future improvements over our current simple prescriptions. Nevertheless, the models faithfully reproduce the number counts and the redshift distributions, and these results can be treated as heuristic guidelines for further investigations.

ACKNOWLEDGMENTS

PH should like to thank Mr. S. Charlot for providing us with their synthesis spectral evolutionary models and helpful correspondences, and Dr. D. Crampton for making the CFRS data available to us in electronic form. We acknowledge the valuable discussion between Dr. B. F. Roukema. We thank Dr. Chris D. Impey for a thorough reading of the first version of this paper, and for his constructive suggestions. We also thank The State Key Laboratory of Science and Engineering Computing (LSEC) of Academia Sinica for providing us with computer supports. This work is in part supported by the National Natural Science Foundation of China.

REFERENCES

Abraham, R.G., Tanvir, N.R., Santiago, B.X., Ellis, R.S., Glazebrook, K., and van den Bergh, S.: 1996, *Mon. Not. R. Astron. Soc.* **279**, L47

Babul, A., and Rees, M.J.: 1992, *Mon. Not. R. Astron. Soc.* **255**, 346

Babul, A., and Ferguson, H.C.: 1996, *Astrophys. J.* **458**, 100

Binggeli, B., Sandage, A., and Tammann, G.A.: 1988, *Annu. Rev. Astron. Astrophys.* **26**, 389

Bower, R., Lucey, J.R., and Ellis, R.S.: 1992, *Mon. Not. R. Astron. Soc.* **254**, 601

Brinchmann, J. et al.: 1998, *Astrophys. J.* **499**, 112

Broadhurst, T.J., Ellis, R.S., and Shanks, T.: 1988, *Mon. Not. R. Astron. Soc.* **235**, 827

Broadhurst, T.J., Ellis, R.S., and Glazebrook, K.: 1992, *Nature* **355**, 55

Bruzual, A.G., and Kron, R.G.: 1980, *Astrophys. J.* **241**, 25

Bruzual, A.G.: 1983, *Astrophys. J.* **273**, 105

Campos, A., and Shanks, T.: 1997, *Mon. Not. R. Astron. Soc.* **291**, 383

Carlberg, R.G., and Charlot, S.: 1992, *Astrophys. J.* **397**, 5

Charlot, S., and Silk, J.: 1994, *Astrophys. J.* **432**, 453

Cole, S., Aragon-Salamanca, A., Frenk, C.S., Navarro, J.F., and Zepf, S.E.: 1994, *Mon. Not. R. Astron. Soc.* **271**, 781

Colin, P., Schramm, D.N., and Peimbert, M.: 1994, *Astrophys. J.* **426**, 459

Colless, M., Ellis, R.S., Taylor, K., and Hook, R.N.: 1990, *Mon. Not. R. Astron. Soc.* **244**, 408

Colless, M., Ellis, R.S., Broadhurst, T.J., Taylor, K., and Bruce, A.: 1993, *Mon. Not. R. Astron. Soc.* **261**, 19

Cowie, L.L.: 1991, *Phys. Scripta* **T36**, 102

Cowie, L.L., Songaila, A., and Hu, E.M.: 1991, *Nature* **354**, 460

Cowie, L.L., Songaila, A., Hu, E.M., and Cohen, J.G.: 1996, *Astron. J.* **112**, 839

Crampton, D., Le Fèvre, O., Lilly, S.J., and Hammer, F.: 1995, *Astrophys. J.* **455**, 96

Disney, M.J.: 1976, *Nature* **263**, 573

Djorgovski, S., Soifer, B.T., Pahre, M.A., Larkin, J.E., Smith, J.D., and Neugebauer, G. et al.: 1995, *Astrophys. J.* **438**, L13

Driver, S.P., Phillipps, S., Davies, J.I., Morgan, I., and Disney, M.J.: 1994, *Mon. Not. R. Astron. Soc.* **266**, 155

Driver, S.P., Windhorst, R.A., and Griffiths, R.E.: 1995, *Astrophys. J.* **453**, 48

Driver, S.P., Windhorst, R.A., Ostrander, E.J., Keel, W.C., Griffiths, R.E., and Ratnatunga, K.U.: 1995, *Astrophys. J.* **449**, L23

Efstathiou, G., Ellis, R.S., and Peterson, B.A.: 1988, *Mon. Not. R. Astron. Soc.* **232**, 431

Ellis, R.S.: 1997, *Annu. Rev. Astron. Astrophys.* **35**, 389

Ferguson, H., and Babul, A.: 1998, *Mon. Not. R. Astron. Soc.* **296**, 585

Ferguson, H., and McGaugh, S.S.: 1995, *Astrophys. J.* **440**, 470

Fritze-v. Alvensleben, U., and Gerhard, O.E.: 1994, *Astron. Astrophys.* **285**, 751

Fukugita, M., Takahara, F., Yamashita, K., and Yoshii, Y.: 1990, *Astrophys. J.* **361**, L1

Gardner, J., Cowie, L.L., and Wainscoat, R.: 1993, *Astrophys. J.* **415**, L9

Gardner, J.P., Sharples, R.M., Frenk, C.S., and Carrasco, B.E.: 1997, *Astrophys. J.* **480**, L99

Glazebrook, K., Peacock, J.A., Collins, C.A., and Miller, L.: 1994, *Mon. Not. R. Astron. Soc.* **266**, 65

Glazebrook, K., Ellis, R.S., Santiago, B.X., and Griffiths, R.: 1995a, *Mon. Not. R. Astron. Soc.* **275**, L19

Glazebrook, K., Peacock, J.A., Miller, J.A., and Collins, C.A.: 1995b, *Mon. Not. R. Astron. Soc.* **275**, 169

Gronwall, C., and Koo, D.C.: 1995, *Astrophys. J.* **440**, L1

Guiderdoni, B., and Rocca-Volmerange, B.: 1990, *Astron. Astrophys.* **227**, 362

Guiderdoni, B., and Rocca-Volmerange, B.: 1991, *Astron. Astrophys.* **252**, 435

Hammer, F., Crampton, D., Le Fèvre, O., and Lilly, S.J.: 1995, *Astrophys. J.* **455**, 88

He, P., and Zhang, Y.Z.: 1998, *Mon. Not. R. Astron. Soc.* **298**, 483 (HZ98)

He, P., and Zhang, Y.Z.: 1999a, *Astrophys. J.* **511**, 574 (HZ99a)

He, P., and Zhang, Y.Z.: 1999b, *Commun. Theor. Phys. (Beijing, China)* **32**, 155

Im, M., Griffiths, R.E., Naim, A., Ratnatunga, K.U., Roche, N., Green, R.F., and Sarajedini, V.L.: 1999, *Astrophys. J.* **510**, 82

Impey, C., and Bothun, G.: 1997, *Annu. Rev. Astron. Astrophys.* **35**, 267

Jones, L.R., Fong, R., Shanks, T., Ellis, R.S., and Peterson, B.A.: 1991, *Mon. Not. R. Astron. Soc.* **249**, 481

Kauffmann, G., White, S.D.M., and Guiderdoni, B.: 1993, *Mon. Not. R. Astron. Soc.* **264**, 201

Kauffmann, G., Guiderdoni, B., and White, S.D.M.: 1994, *Mon. Not. R. Astron. Soc.* **267**, 981

Kauffmann, G., Charlot, S., and White, S.D.M.: 1996, *Mon. Not. R. Astron. Soc.* **283**, L117

Koo, D.C.: 1981, PhD Thesis, Univ. of California, Berkeley

Koo, D.C.: 1985, *Astron. J.* **90**, 418

Koo, D.C., and Kron, R.G.: 1992, *Annu. Rev. Astron. Astrophys.* **30**, 613

Le Fèvre, O., Crampton, D., Lilly, S.J., Hammer, F., and Tresse, L.: 1995, *Astrophys. J.* **455**, 60

Lilly, S.J., Cowie, L.L., and Gardner, J.P.: 1991, *Astrophys. J.* **369**, 79

Lilly, S.J., Le Fèvre, O., Crampton, D., Hammer, F., and Tresse, L.: 1995a, *Astrophys. J.* **455**, 50

Lilly, S.J., Hammer, F., Le Fèvre, O., and Crampton, D.: 1995b, *Astrophys. J.* **455**, 75

Lilly, S.J., et al.: 1998, *Astrophys. J.* **500**, 75

Loveday, J., Peterson, B.A., Efstathiou, G., and Maddox, S.J.: 1992, *Astrophys. J.* **390**, 338

Madau, P.: 1995, *Astrophys. J.* **441**, 18

Maddox, S.J., Efstathiou, G., Sutherland, W.J., and Loveday, J.: 1990a, *Mon. Not. R. Astron. Soc.* **243**, 692

Maddox, S.J., Sutherland, W.J., Efstathiou, G., Loveday, J., and Peterson, B.A.: 1990b, *Mon. Not. R. Astron. Soc.* **247**, 1p

Marzke, R.O., Geller, M.J., Huchra, J.P., and Corwin Jr., H.G.: 1994, *Astron. J.* **108**, 437

McLeod, B.A., Bernstein, G.M., Rieke, M.J., Tolstrup, E.V., and Fazio, G.G.: 1995, *Astrophys. J. Suppl.* **96**, 117

Metcalfe, N., Shanks, T., Fong, R., and Jones, L.R.: 1991, *Mon. Not. R. Astron. Soc.* **249**, 498

Metcalfe, N., Fong, R., and Shanks, T.: 1995a, *Mon. Not. R. Astron. Soc.* **274**, 769

Metcalfe, N., Shanks, T., Fong, R., and Roche, N.: 1995b, *Mon. Not. R. Astron. Soc.* **273**, 257

Metcalfe, N., Shanks, T., Campos, A., Fong, R., and Gardner, J.P.: 1996, *Nature* **383**, 236

Mobasher, B., Ellis, R.S., and Sharples, R.M.: 1986, *Mon. Not. R. Astron. Soc.* **223**, 11

Moustakas, L.A., Davis, M., Graham, J.R., Silk, J., Peterson, B.A., and Yoshii, Y.: 1997, *Astrophys. J.* **475**, 445

Pozzetti, L., Bruzual, A.G., and Zamorani, G.: 1996, *Mon. Not. R. Astron. Soc.* **281**, 953

Rocca-Volmerange, B., and Guiderdoni, B.: 1990, *Mon. Not. R. Astron. Soc.* **247**, 166

Roukema, B.F., and Yoshii, Y.: 1993, *Astrophys. J.* **418**, L1

Roukema, B.F., Peterson, B.A., Quinn, P.J., and Rocca-Volmerange, B.: 1997, *Mon. Not. R. Astron. Soc.* **292**, 835

Salpeter, E.E.: 1955, *Astrophys. J.* **121**, 161

Scalo, J.M.: 1986, *Fundam. Cosmic Phys.* **11**, 1

Schechter, P.: 1976, *Astrophys. J.* **203**, 297

Schmidt, M.: 1968, *Astrophys. J.* **151**, 393

Shanks, T.: 1989, in The Extra-Galactic Background Light, eds. S. C. Bowyer & C. Leinert (Kluwer Academic Publishers), p.269

Soifer, B.T., Matthews, K., Djorgovski, S., Larkin, J., Graham, J.R., Harrison, W., Jernigan, G., and Lin, S. et al.: 1994, *Astrophys. J.* **420**, L1

Steidel, C.C., and Hamilton, D.: 1992, *Astron. J.* **104**, 941

Steidel, C.C., and Hamilton, D.: 1993, *Astron. J.* **105**, 2017

Steidel, C.C., Pettini, M., and Hamilton, D.: 1995, *Astron. J.* **110**, 2519

Steidel, C.C., Giavalisco, M., Pettini, M., Dickinson, M., and Adelberger, K.L.: 1996, *Astrophys. J.* **462**, L17

Steidel, C.C., Adelberger, K.L., Dickinson, M., Giavalisco, M., Pettini, M., and Kellogg, M.: 1998, *Astrophys. J.* **492**, 428

Stevenson, P.R.F., Shanks, T., and Fong, R.: 1986, in Spectral Evolution of Galaxies., eds. C. Chiosi & A. Renzini (Reidel, Dordrecht), p.439

Szokoly, G.P., Subbarao, M.U., Connolly, A.J., and Mobasher, B.: 1998, *Astrophys. J.* **492**, 452

Tinsley, B.M.: 1980, *Astrophys. J.* **241**, 41

Teplitz, H.I., Gardner, J.P., Malumuth, E.M., and Heap, S.R.: 1998, *Astrophys. J.* **507**, L17

Totani, T., and Yoshii, Y.: 1998, *Astrophys. J.* **501**, L177

Tyson, J.A.: 1988, *Astron. J.* **96**, 1

Wang, B.: 1991, *Astrophys. J.* **383**, L37

Woods, D., and Fahlman, G.G.: 1997, *Astrophys. J.* **490**, 11

Worley, G.: 1994, *Astrophys. J. Suppl.* **95**, 107

Zepf, S.E.: 1997, *Nature* **390**, 377

Zucca, E., Zamorani, G., Vettolani, G., Cappi, A., Merighi, R., Mignoli, M., Stirpe, G.M., and MacGillivray, H. et al.: 1997, *Astron. Astrophys.* **326**, 477

Zwicky, F.: 1957, in Morphological Astronomy, Springer-Verlag

TABLE 1
 B -BAND LF PARAMETERS FOR PRESENT-DAY GALAXIES.

	E/S0	Sab	Sbc	Scd	Sdm/Irr	vB
ϕ^*	10.0	4.00	6.00	6.00	4.00	4.00
M^*	-21.0	-20.80	-20.80	-20.80	-20.70	-20.50
α	-0.90	-0.95	-1.10	-1.10	-1.20	-1.30

Notes:

- (1). ϕ^* , M^* , and α are determined by trial and error, see text for details;
- (2). ϕ^* in units of $10^{-4}/\text{Mpc}^3$;
- (3). vB galaxies, taken after Pozzetti et al. (1996), are included to explain the bluest samples, e.g., CFRS. See text for details;
- (4). The Hubble constant has been scaled to $h=0.5$.

TABLE 2
SFR PARAMETER τ_e (MEASURED IN GYR) AND MODELLED $B - I$ AND $B - K$ COLORS FOR GALAXIES IN THE THREE COSMOLOGICAL MODELS UNDER CONSIDERATION.

Type	Scen. A			Scen. B			Scen. C		
	τ_e	$B - I$	$B - K$	τ_e	$B - I$	$B - K$	τ_e	$B - I$	$B - K$
E/S0-I	0.5	2.29	4.14	1.0	2.34	4.17	1.1	2.35	4.18
E/S0-II	0.7	2.29	4.12	1.4	2.33	4.16	1.6	2.33	4.16
E/S0-III	1.0	2.28	4.11	2.1	2.30	4.11	2.4	2.30	4.10
E/S0-IV	1.5	2.25	4.07	3.0	2.24	4.06	3.1	2.24	4.07
E/S0-V	2.1	2.21	4.00	4.1	2.15	3.94	4.3	2.15	3.94
Sab	2.3	2.15	3.89	3.3	2.17	3.93	3.5	2.15	3.91
Sbc	4.6	1.81	3.45	6.3	1.84	3.51	7.0	1.81	3.47
Scd	9.5	1.57	3.14	13.5	1.60	3.19	15.0	1.59	3.18
Sdm/Irr	∞	1.37	2.87	∞	1.42	2.95	∞	1.43	2.96
vB	-	0.92	2.25	-	0.92	2.25	-	0.92	2.25

Notes:

- (1). We choose a Scalo IMF for ellipticals, and a Salpeter IMF for the other types;
- (2). $\tau_e = \infty$ for Sdm/Irr galaxies denotes constant SFR;
- (3). The SFR of vB galaxies is not described by Eq. [1]. See text for detail.

TABLE 3

THE PHENOMENOLOGICAL PARAMETERS FOR THE NUMBER EVOLUTION MODELS IN THE THREE COSMOLOGICAL MODELS UNDER CONSIDERATION.

Parameter	E/S0	Sab	Sbc	Scd	Sdm/Irr	vB
Scen. A						
Q_0	-0.02	0	0	0	1.0	1.0
Q_2	-0.05	0.03	0.03	0.03	0.03	0.03
γ_1	0	0.2	0.2	0.2	0.2	0.2
γ_2	0	0.5	0.5	0.5	0.5	0.5
Scen. B						
Q_0	-0.05	0	0	0	—	—
Q_2	-0.15	0	0	0	—	—
γ_1	0	0.2	0.2	0.2	0.2	0.2
γ_2	0	0.4	0.4	0.4	0.4	0.4
Scen. C						
Q_0	-0.2	0	0	0	—	—
Q_2	-0.15	0	0	0	—	—
γ_1	0	0.2	0.2	0.2	0.2	0.2
γ_2	0	0.4	0.4	0.4	0.4	0.4

Notes:

Q_0 and Q_2 for Sdm/Irr and vB galaxies in Scenarios B and C are determined by Eq. [4].

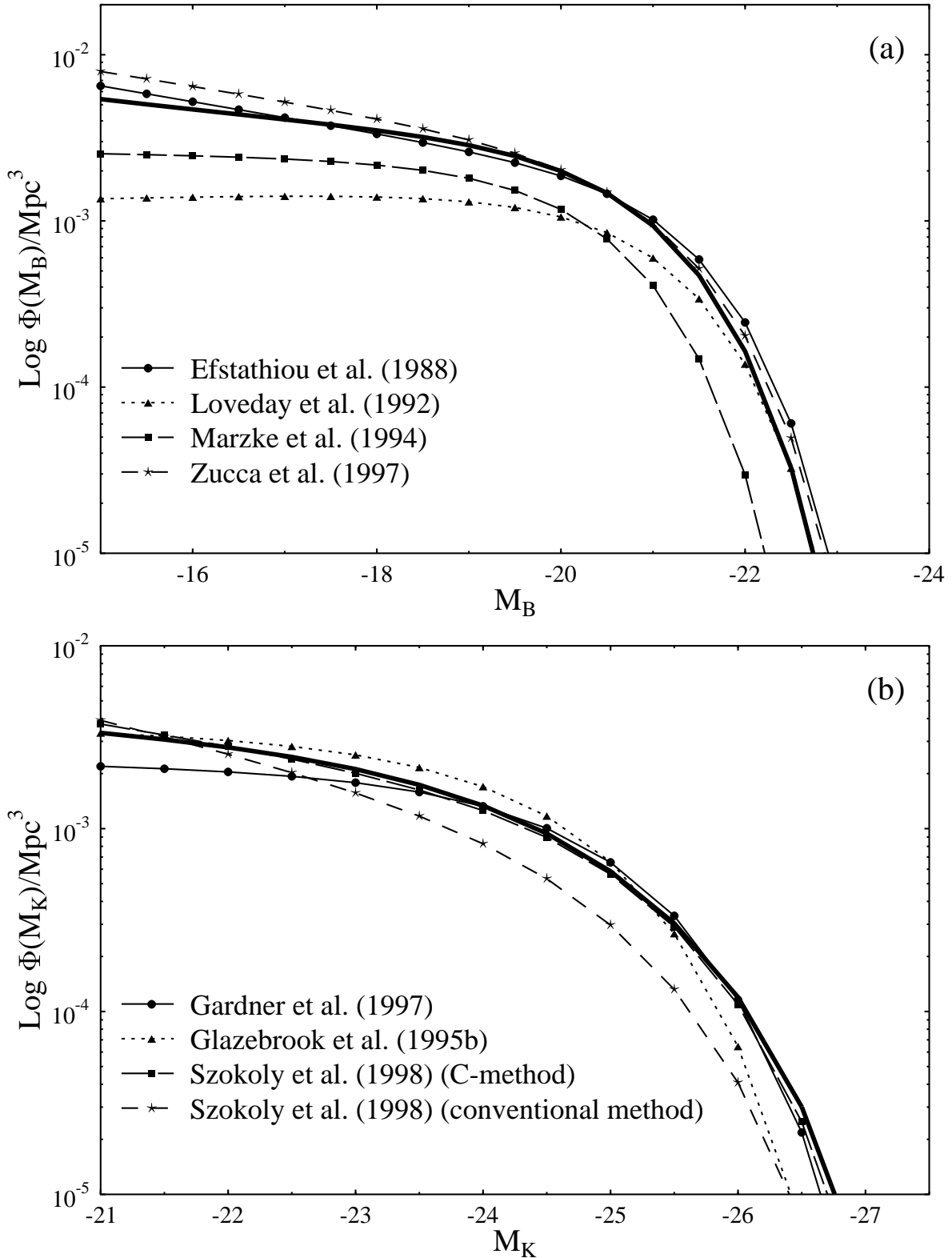


FIG. 1.— Present-day luminosity functions of galaxies. The adopted LFs are indicated by thick lines, whose values correspond to those in Table 1. Here and hereafter, the capital letters A, B and C refer to Scenarios A, B and C, respectively. Observational data were obtained as follows. (a) Solid line with dots: Efstathiou, Ellis, & Peterson (1988), dotted line with triangles: Loveday et al. (1992), dashed line with squares: Marzke et al. (1994), dashed line with stars: Zucca et al. (1997). (b) Solid line with dots: Gardner et al. (1997), dotted line with triangles: Glazebrook et al. (1995b), dashed line with squares: Szokoly et al. (1998; C-method), dashed line with stars: Szokoly et al. (1998; conventional method). Notice that the characteristic density ϕ^* and the mixing ratio between different galaxies of Efstathiou et al. (1988) LF are taken from Pozzetti et al. (1996). Panels (a) and (b) are for B and K bands, respectively. The Hubble constant has been scaled to $h = 0.5$ for Scenario C.

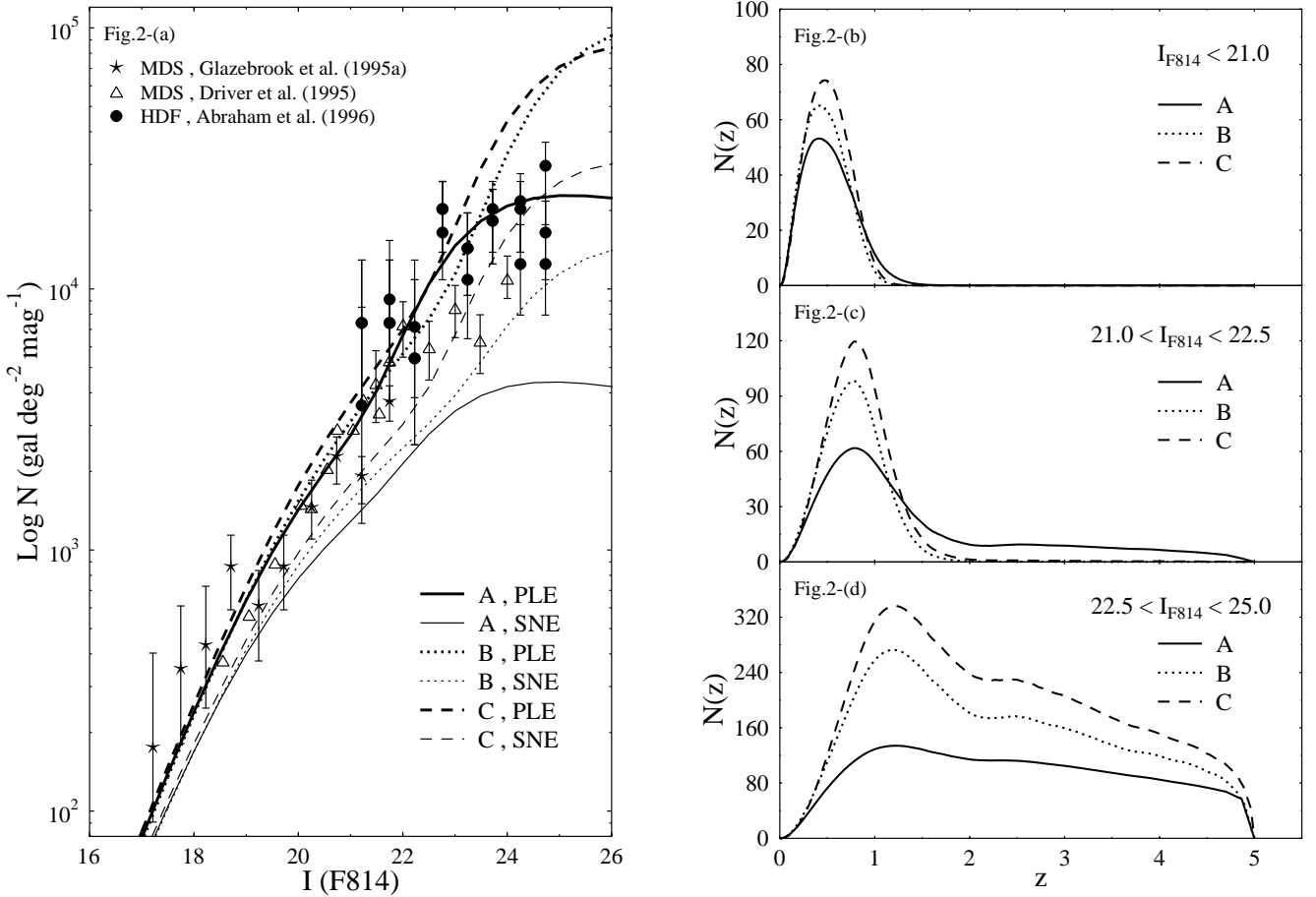


FIG. 2.— (a). Differential number counts for E/S0 galaxies as a function of apparent magnitude in I_{814} band. The sources of the observational data are exhibited in the figure and these data are indicated by symbols. The model predictions are shown by lines. ‘PLE’ denotes pure luminosity evolution models, and ‘SNE’, predictions of the strong number evolution, based on the formalism of Kauffmann et al. (1996). See Section 2.1 for details. Fig.2-(b), (c), and (d) are the z distributions for E/S0 limited to three magnitude bins, $I_{814} < 21.0$, $21.0 < I_{814} < 22.5$ and $22.5 < I_{814} < 25.0$, respectively. Models are indicated by lines, and the model predictions have been normalized in units of deg^{-2} with a redshift bin $\Delta z = 0.01$.

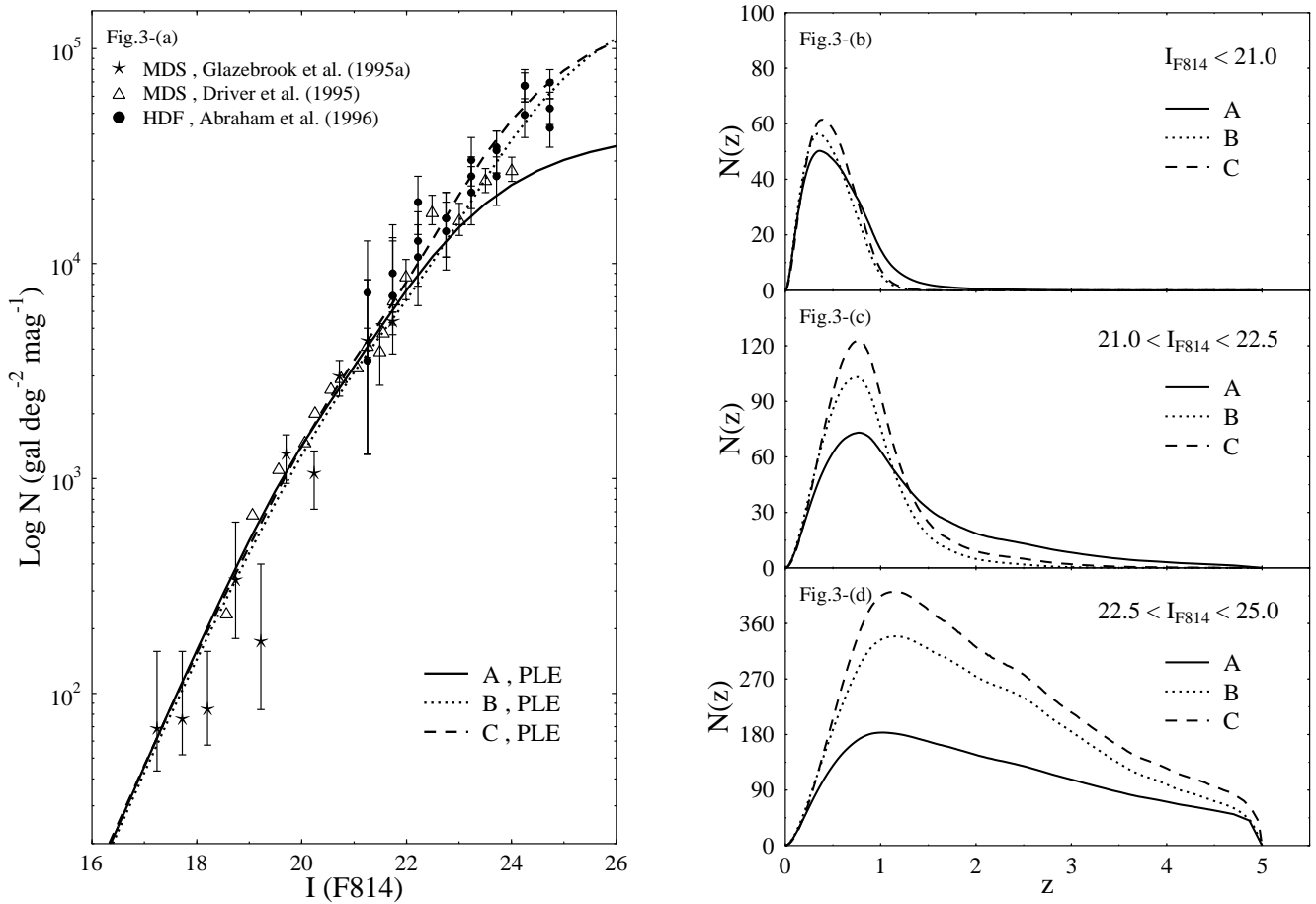


FIG. 3.— The same as Figure 2, but for early-type spiral galaxies (Sab+Sbc).

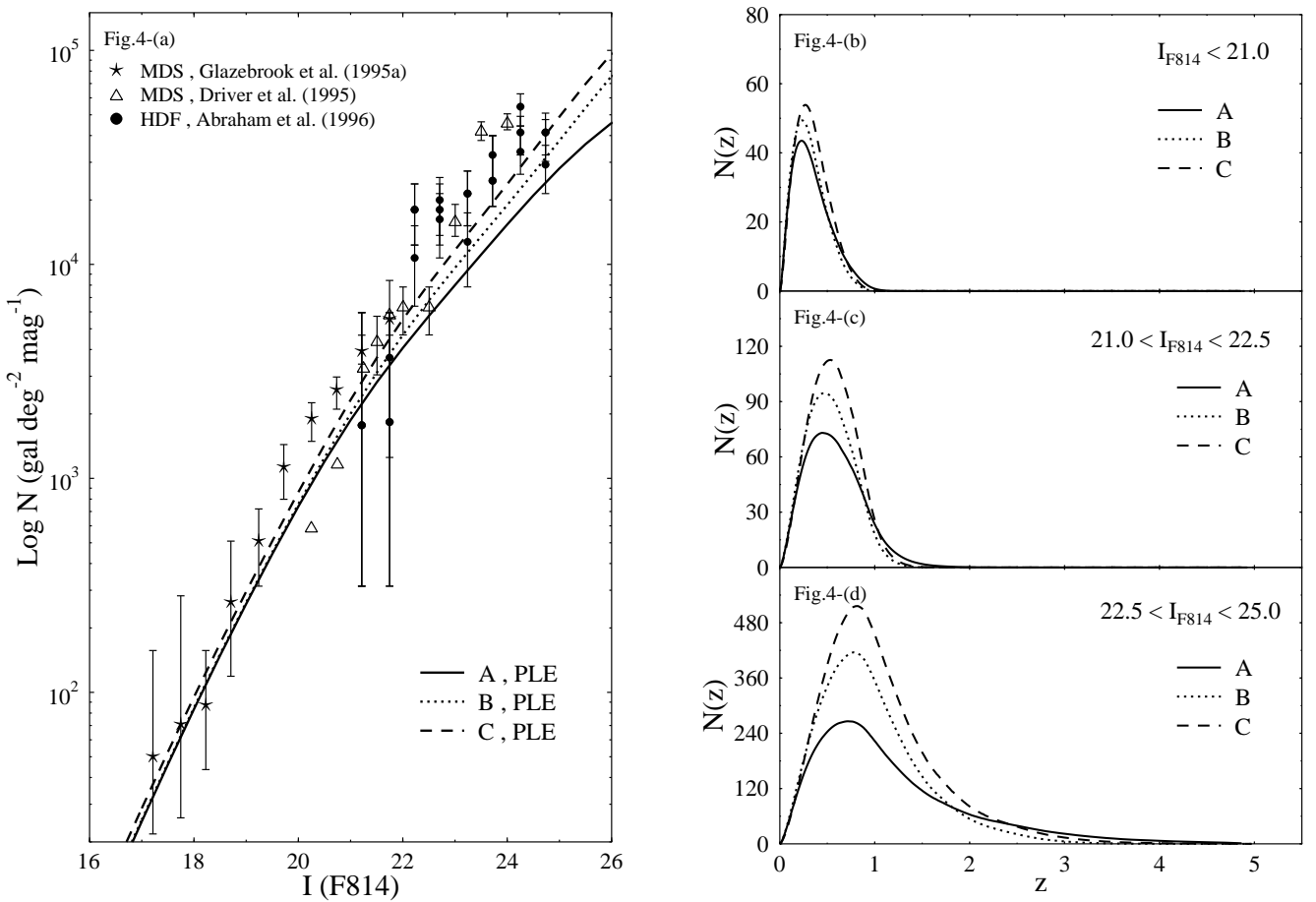


FIG. 4.— The same as Figure 2 and 3, but for late-type spiral/irregular (Scd+Sdm/Irr) and vB galaxies.

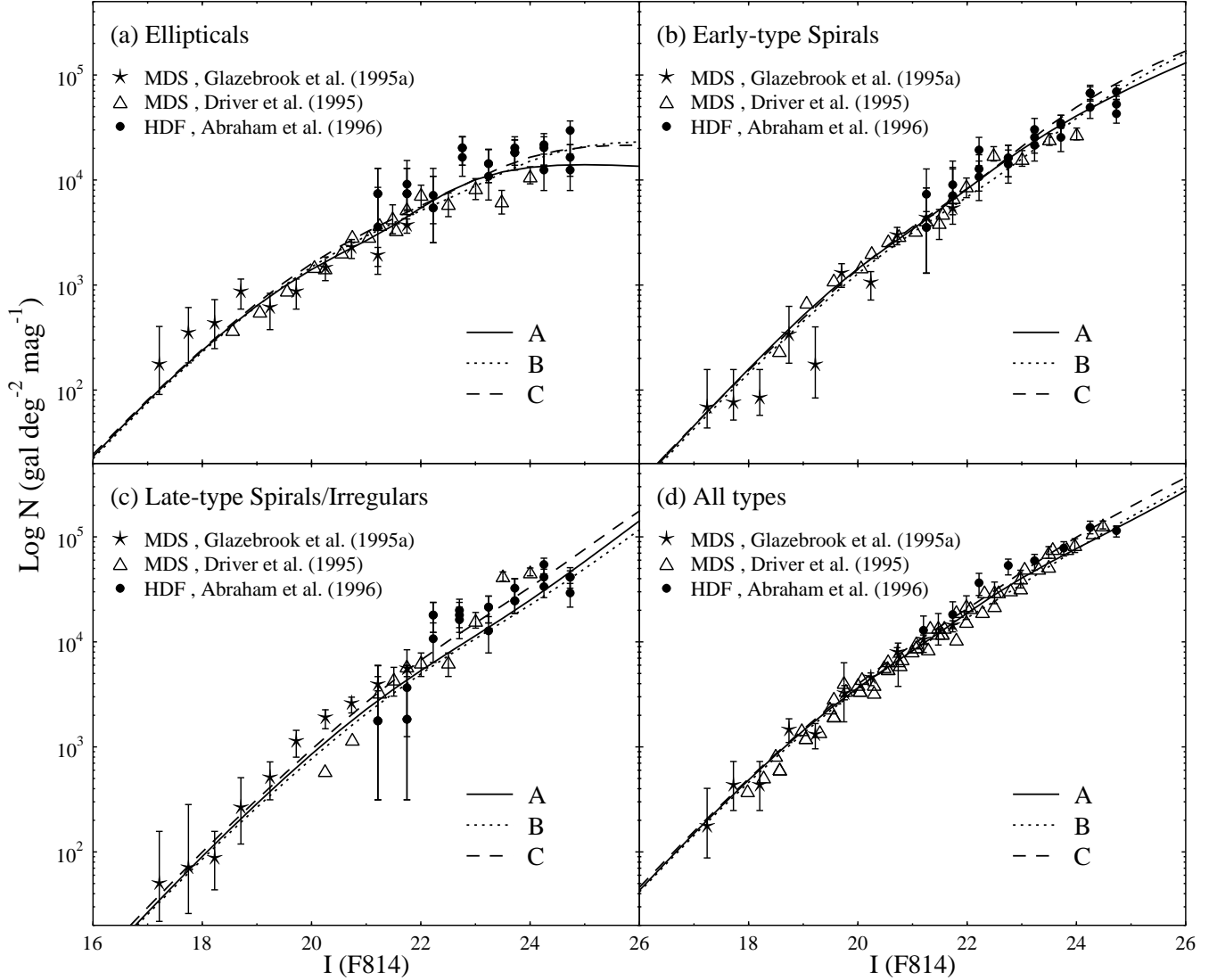


FIG. 5.— Differential number counts for galaxies as a function of apparent magnitude in I_{814} band. Panel (a), (b), (c) and (d) are for ellipticals, early-type spirals, late-type spiral/irregular/vB galaxies and the overall population, respectively. The model predictions are shown by lines.

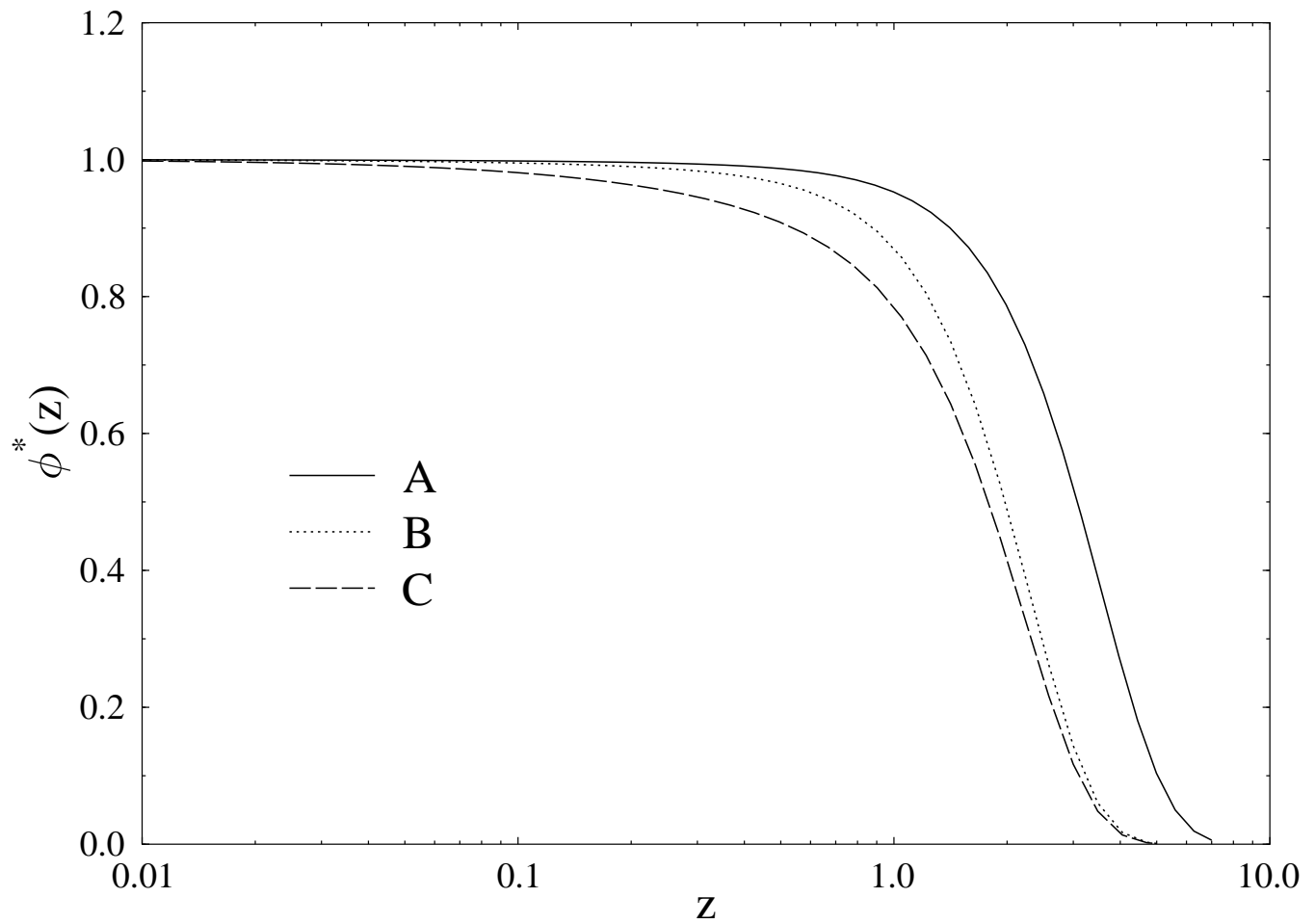


FIG. 6.— The evolution of the characteristic number density ϕ^* of E/S0 galaxies with respect to z . ϕ^* is normalized to unity at the present day.

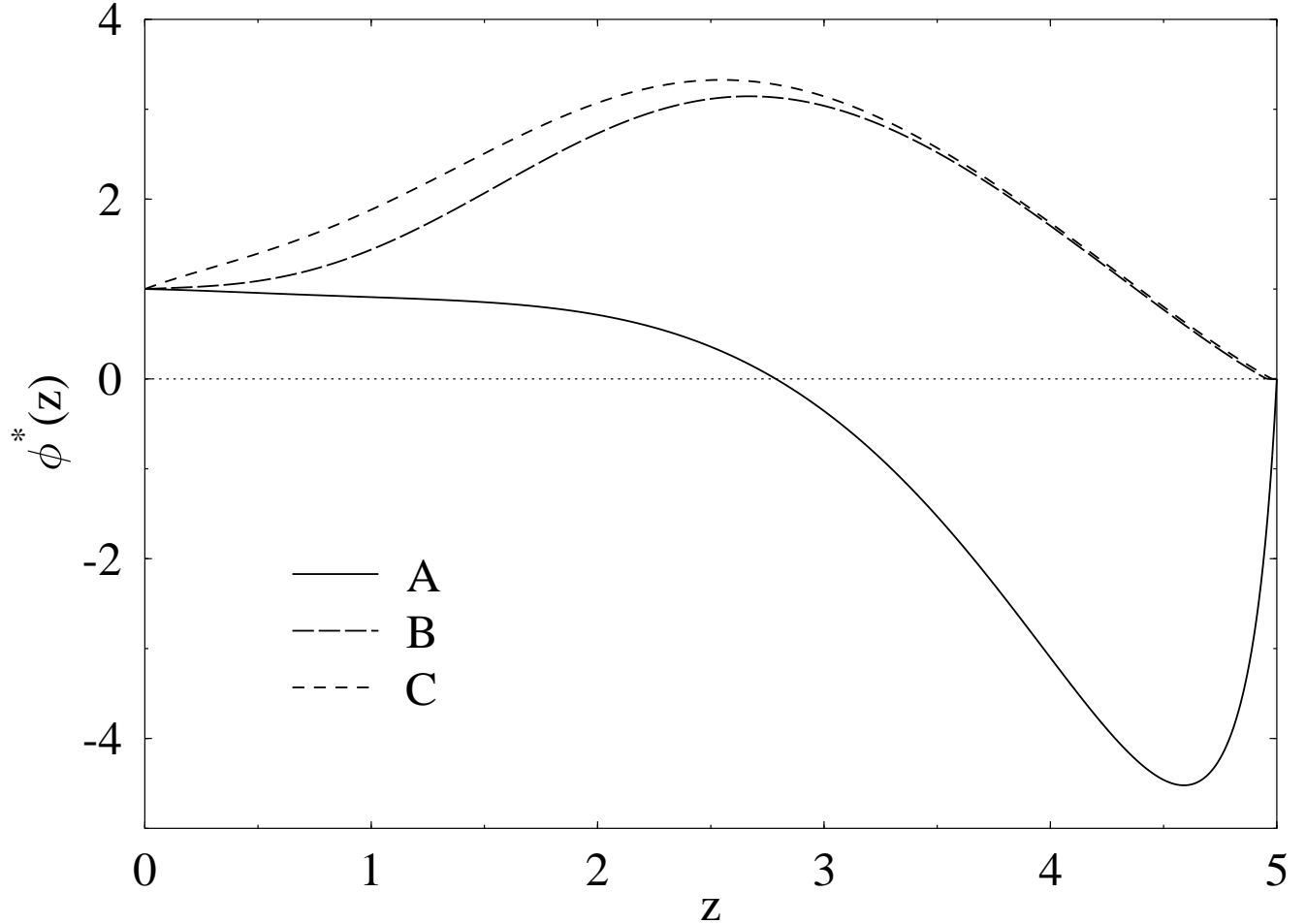


FIG. 7.— The evolution of the characteristic number density ϕ^* of Sdm/Irr and vB galaxies with respect to z , constrained by the conservation of the comoving mass density, Eq. [4]. ϕ^* is normalized to unity at the present day.

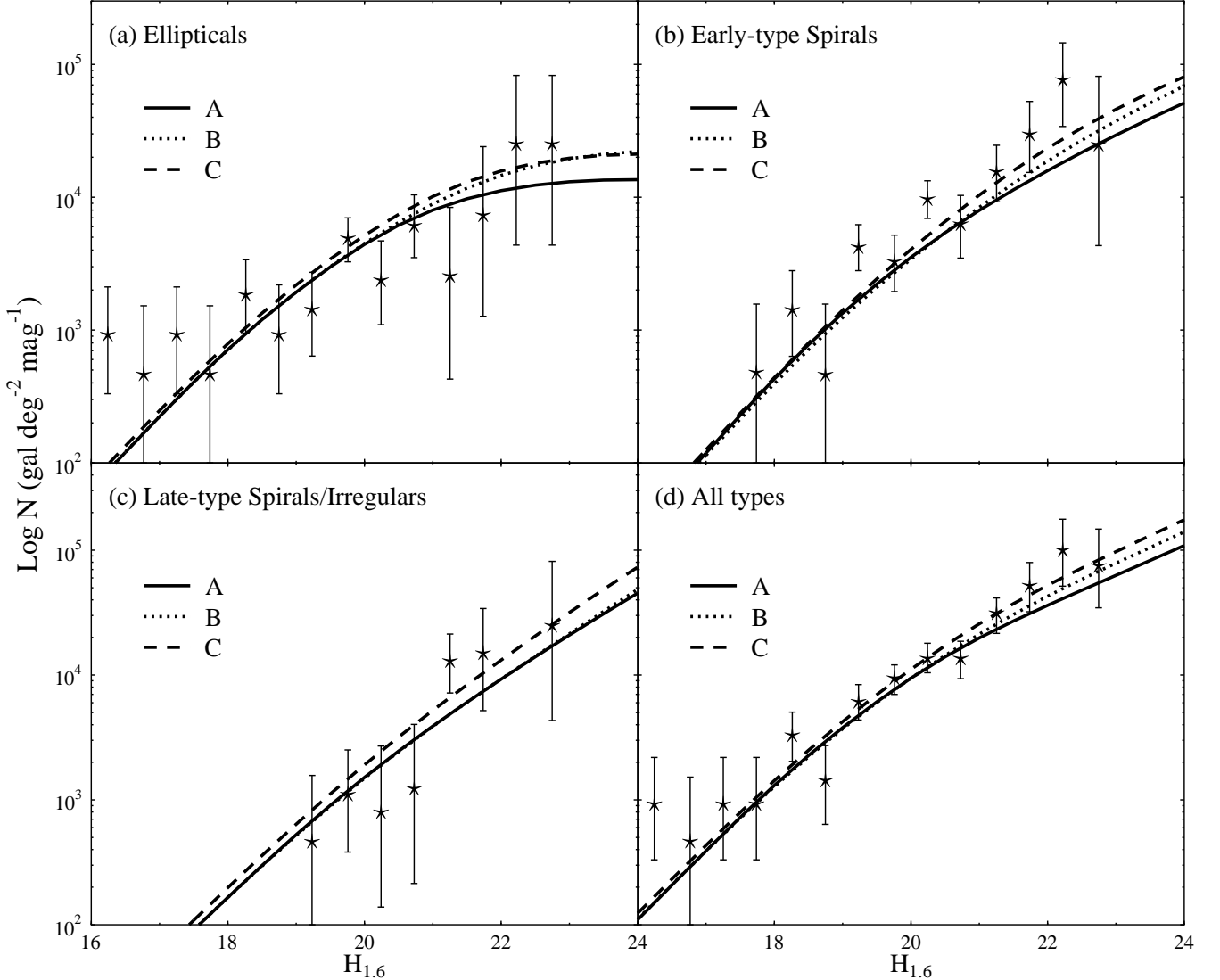


FIG. 8.— Differential number counts for galaxies as a function of apparent magnitude in $H_{1.6}$ band. Panel (a), (b), (c) and (d) are for ellipticals, early-type spirals, late-type spiral/irregular/vB galaxies and the overall population, respectively. The data are taken from NICMOS (Teplitz et al. 1998); the model predictions are shown by lines.

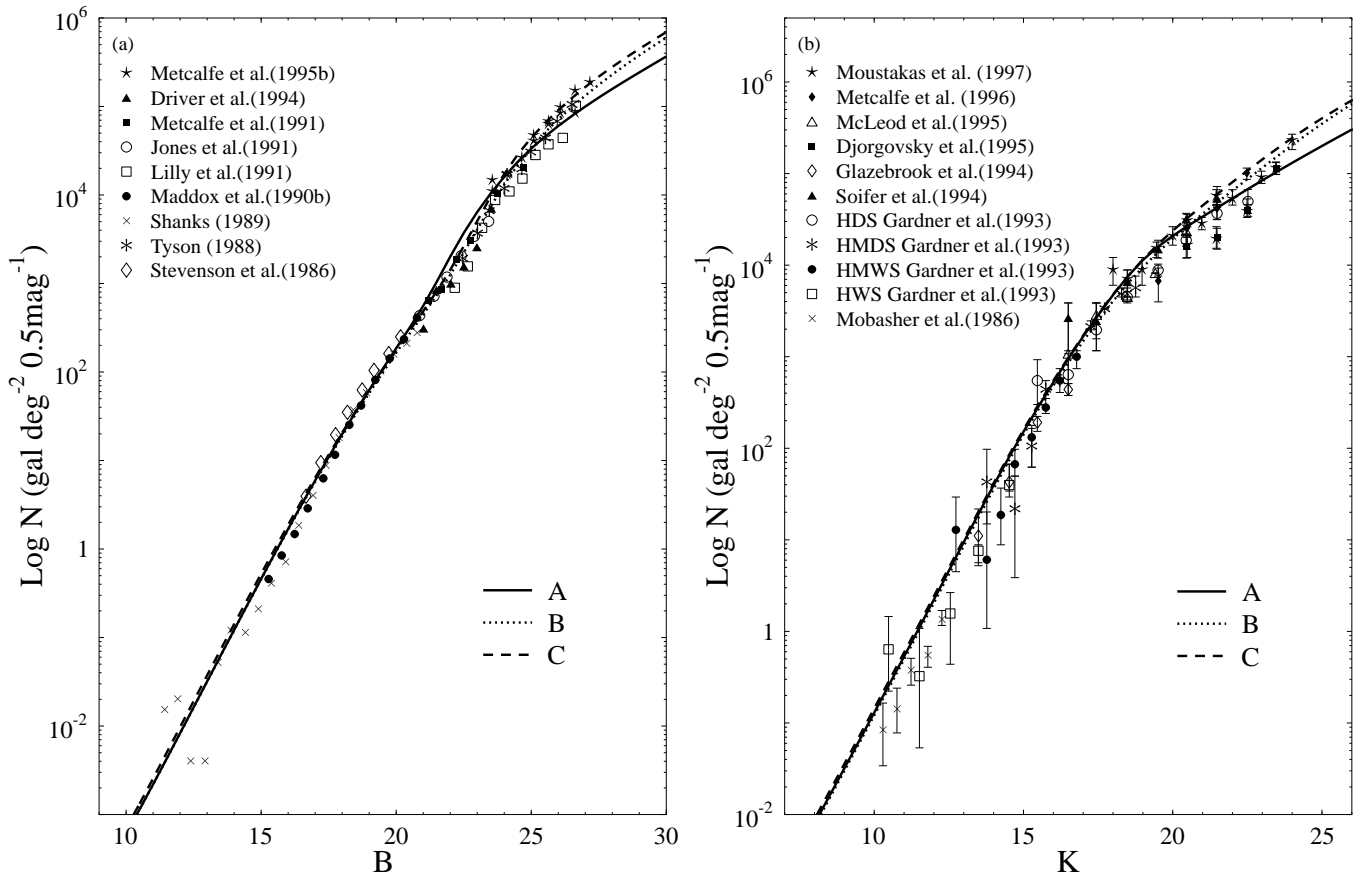


FIG. 9.— Differential number counts as a function of apparent magnitude in B - and K - bands. The sources of observational data are exhibited in the figure. Model predictions are shown by lines.

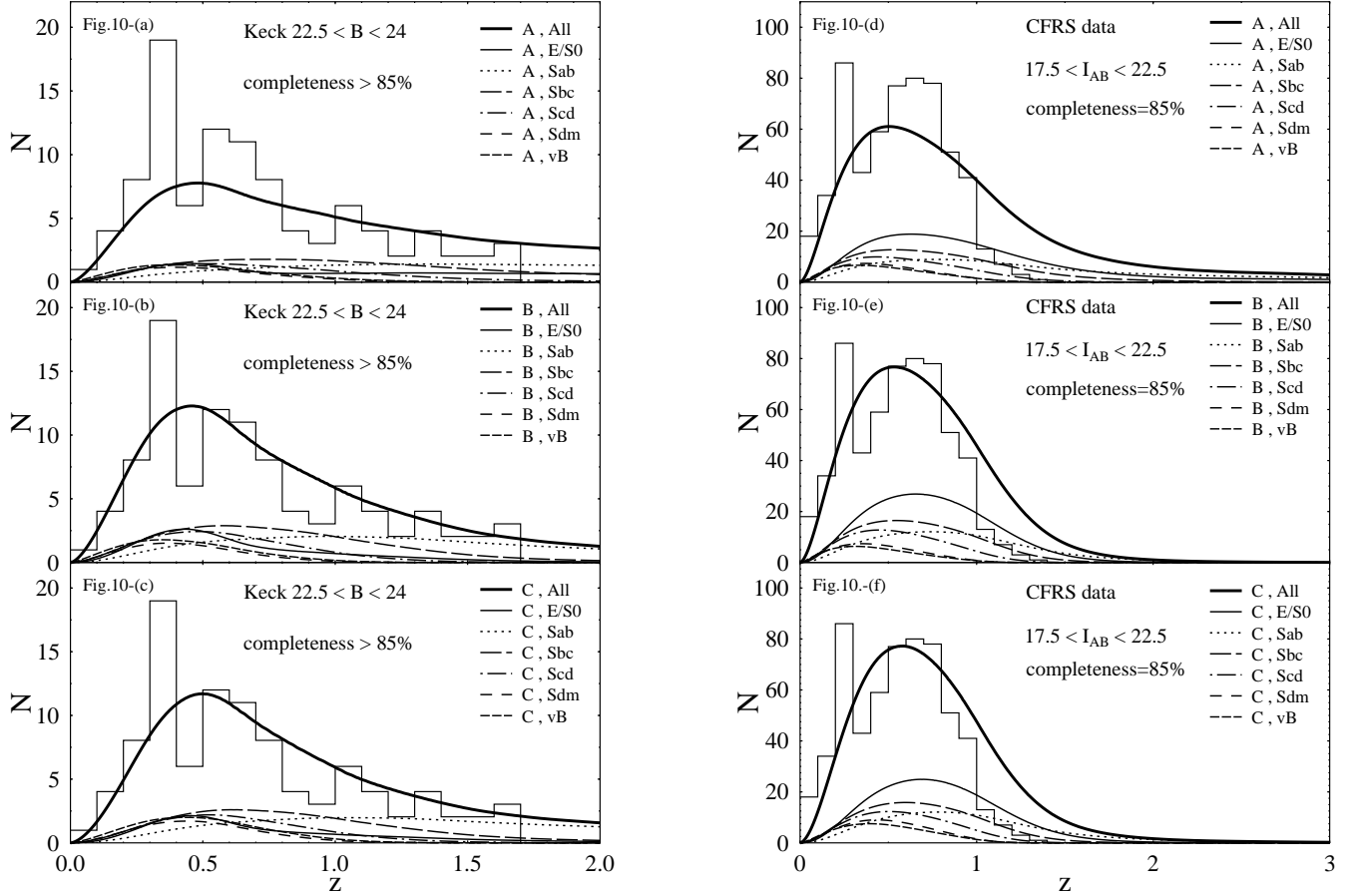


FIG. 10.— The z distributions for galaxies. Fig.10-(a), (b), and (c) are limited in the magnitude range of $22.5 < B < 24.0$, and for Scenario A, B, and C, respectively. Fig.10-(d), (e), and (f) are corresponding to (a), (b), and (c), respectively, but are limited in $17.5 < I_{AB} < 22.5$. The sources of the observed data are indicated in the figure, and they are shown by histograms. Model predictions are indicated by lines, which have been normalized to give the total number of both z -identified and z -unidentified objects.